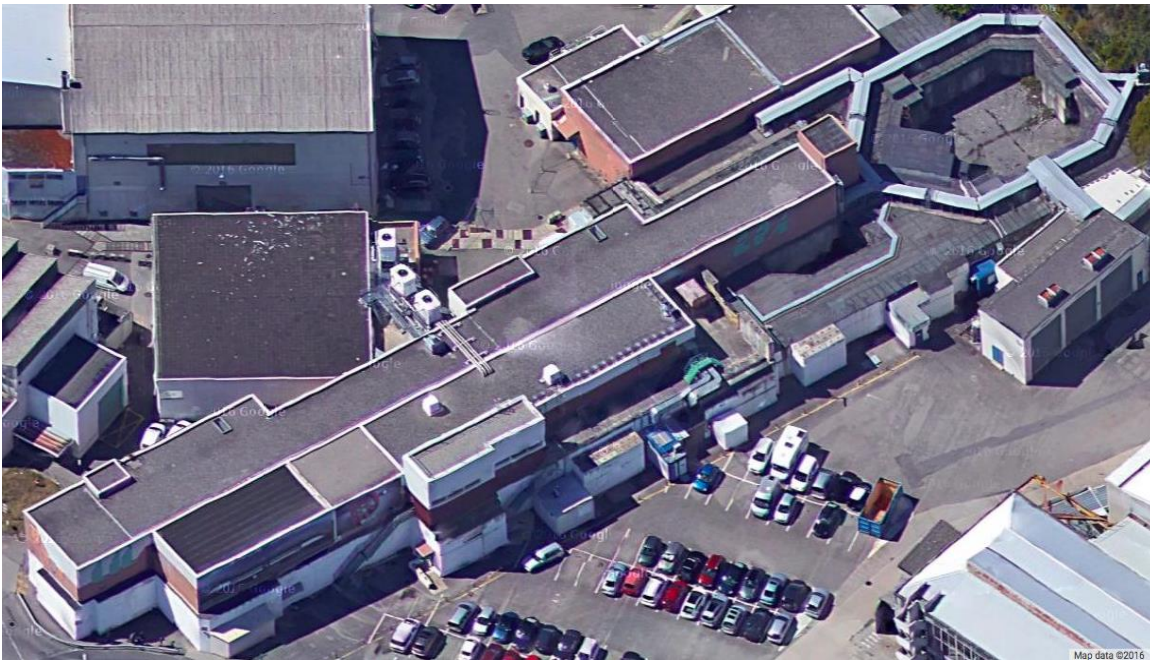


8 Performance	233
8.1 Introduction	234
8.2 Drive Beam Generation, Power Production and Two-Beam Acceleration in the CLIC Test Facility CTF3	236
8.3 Drive Beam Injector Performance	243
8.4 BDS Beam Dynamics, Experimental Studies in ATF2 and FFTB	245
8.5 Low Emittance Preservation (FACET / Elettra)	247
8.6 Performance of High-Gradient RF systems	251
8.7 Damping Rings	255
8.8 Impact of Stray Magnetic Fields	259

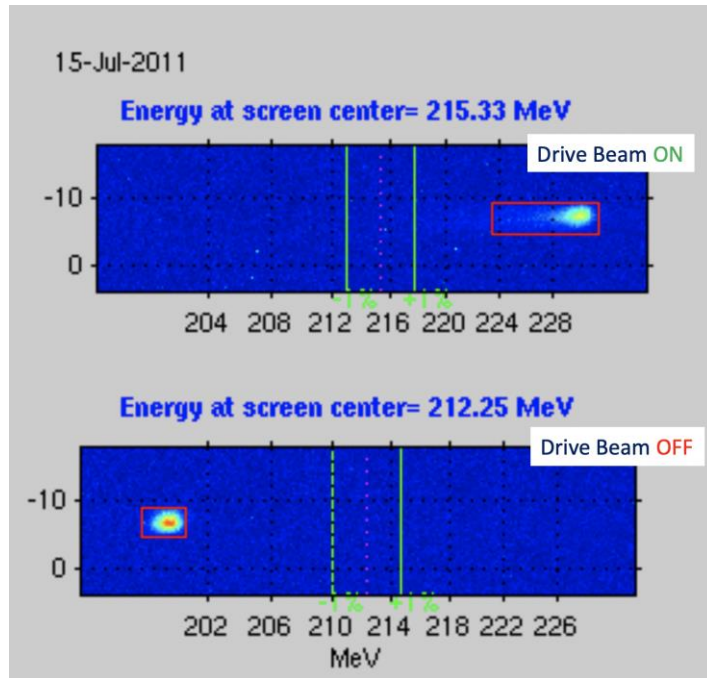


Status: In principle final.

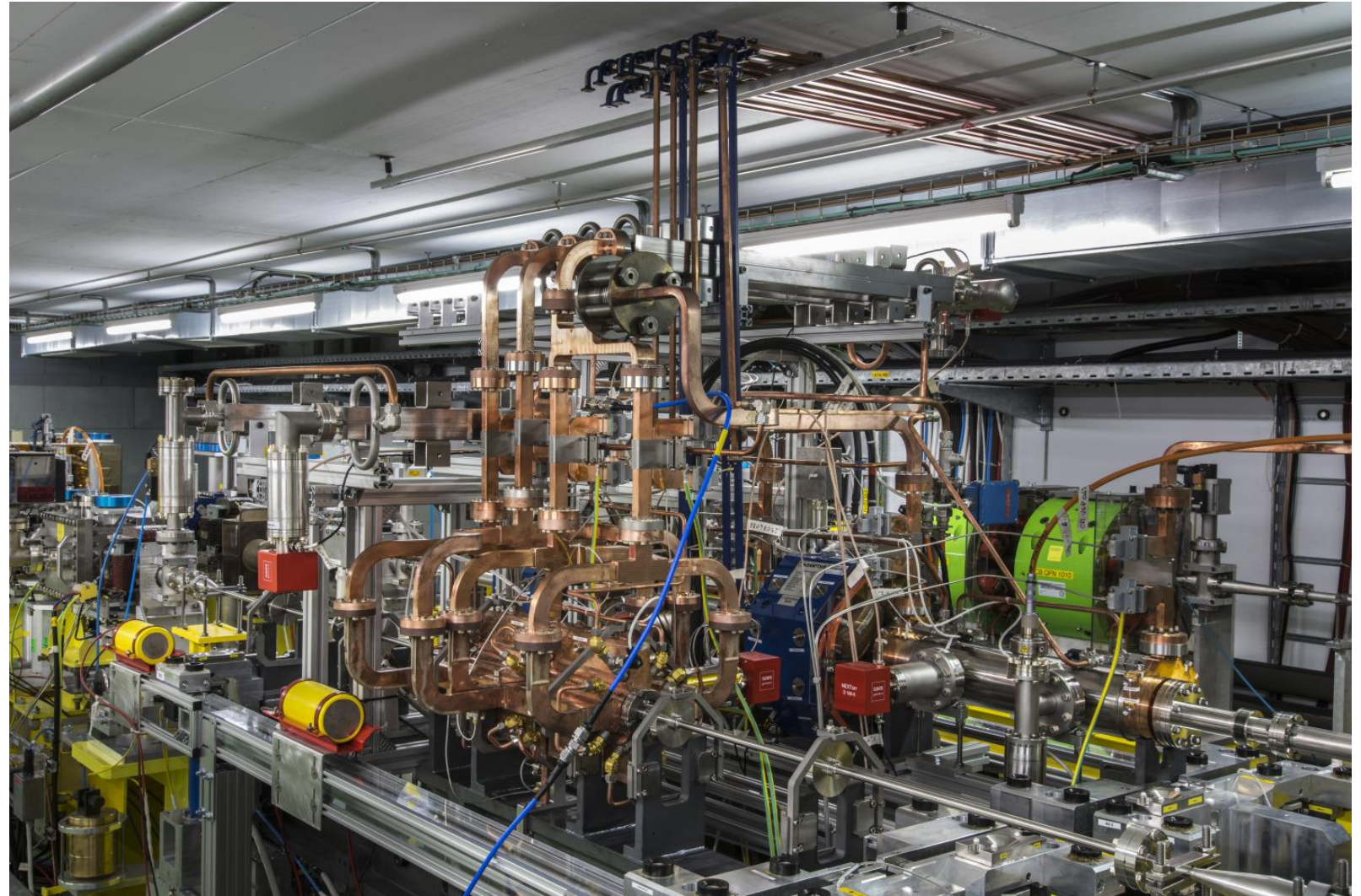
Thanks to all contributing authors (Daniel, Phil, Steffen, Rogelio, Andrea, Walter, Nuria, Gerry, Yannis, Edu, Chetan.)

But, above all, thanks to all people who contributed to the documented results over many years...

Drive Beam Generation, Power Production and Two-Beam Acceleration in CTF3



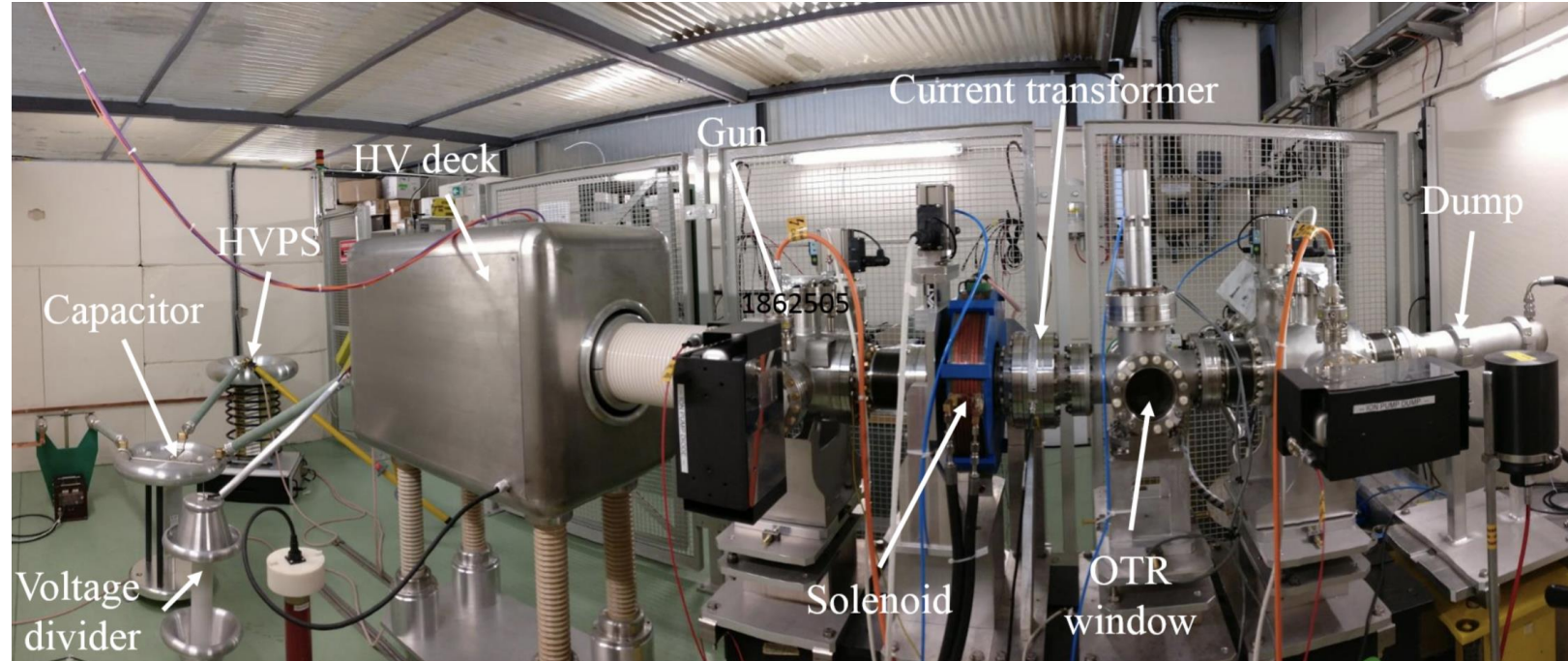
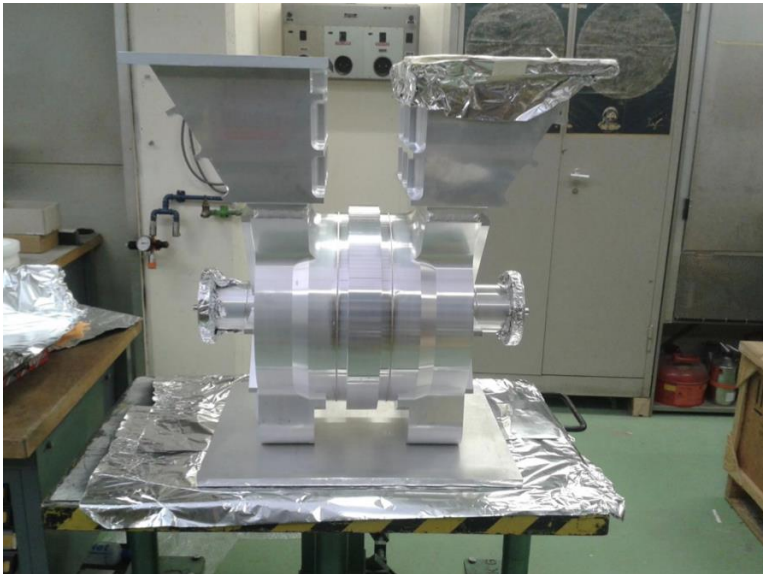
Probe Beam observed in the TBTS spectrometer screen with the 12 GHz RF power from the drive beam on (top) and off (bottom). The energy gain is about 32 MeV, corresponding to a gradient of 145 MV/m.



The Two-Beam Module, TBM, a 2 m long fully representative unit of the CLIC main linac, installed in the CLEX area of CTF3.

Drive Beam Injector Performance

Prototype of a 500 MHz sub-harmonic buncher for the CLIC drive beam injector. The cavity was made of aluminum.



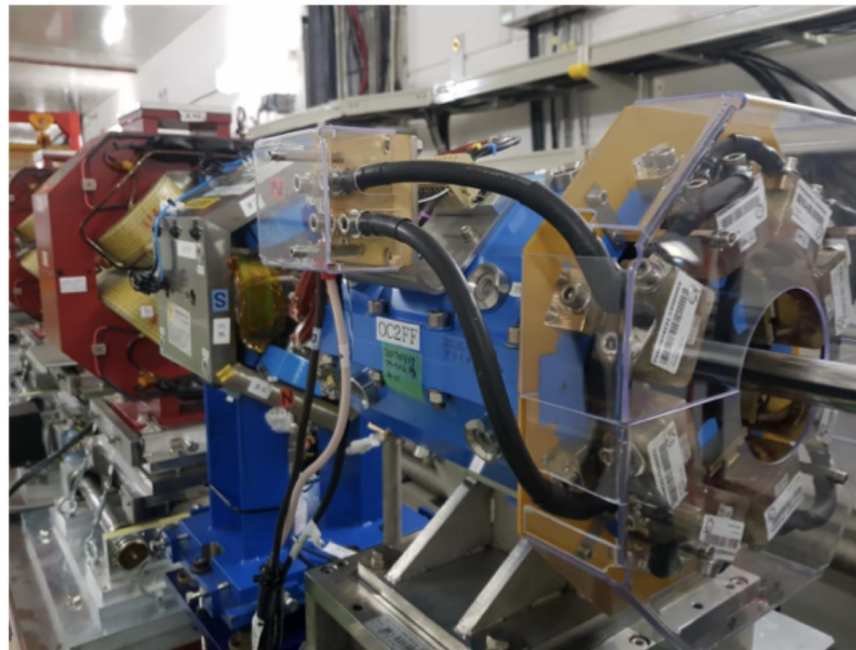
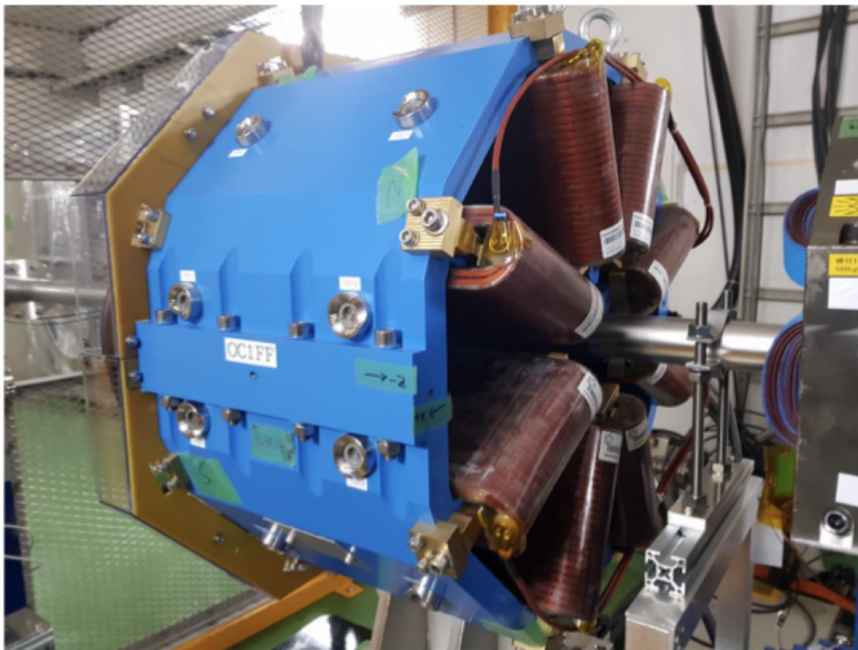
Drive Beam Electron Source test stand at CERN. The cathode is installed within a ceramic insulator while the anode is on ground potential. All drive electronics for the cathode is installed on a high voltage deck at a potential of 140 kV. The beam can be diagnosed to measure its current, shape and emittance.

BDS Beam Dynamics, Experimental Studies in ATF2 and FFTB

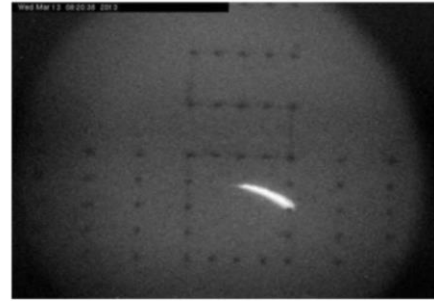
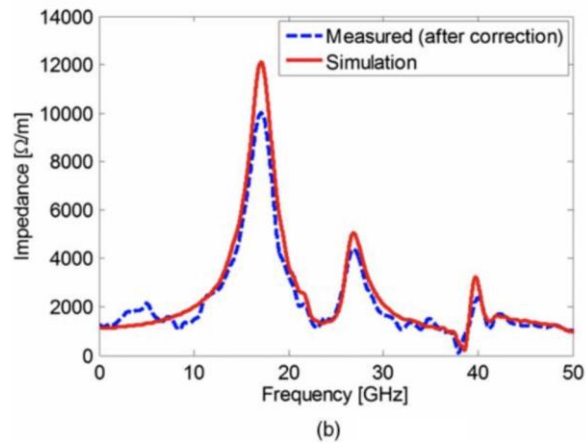
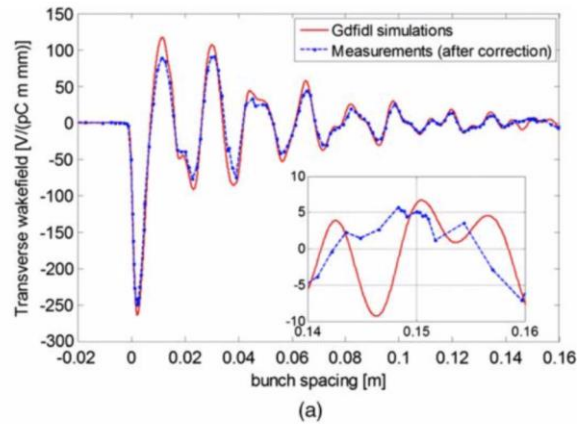
Table 8.1: FFS parameters for CLIC and related experimental projects [30–36].

	CLIC 3 TeV	FFTB	ATF2			SKEKB Low β^*
			Nom.	UL β^*	Long L^*	
L^* [m]	6	0.4	1	1	2	0.9
β_y^* [mm]	0.12	0.1	0.1	0.025	0.1	0.09
$\xi_y \approx L^*/\beta_y^*$ [10^3]	50	4	10	40	20	10
ϵ_y [pm]	0.003	22	12	12	12	13
σ_y design [nm]	1	52	37	23	37	34
σ_y measured [nm]	-	70±6	41±2	-	-	-

Octupole magnets OCT1 (left) and OCT2 (right) installed at ATF2 beamline.



Low Emittance Preservation (FACET / Elettra)



iteration 0



iteration 1



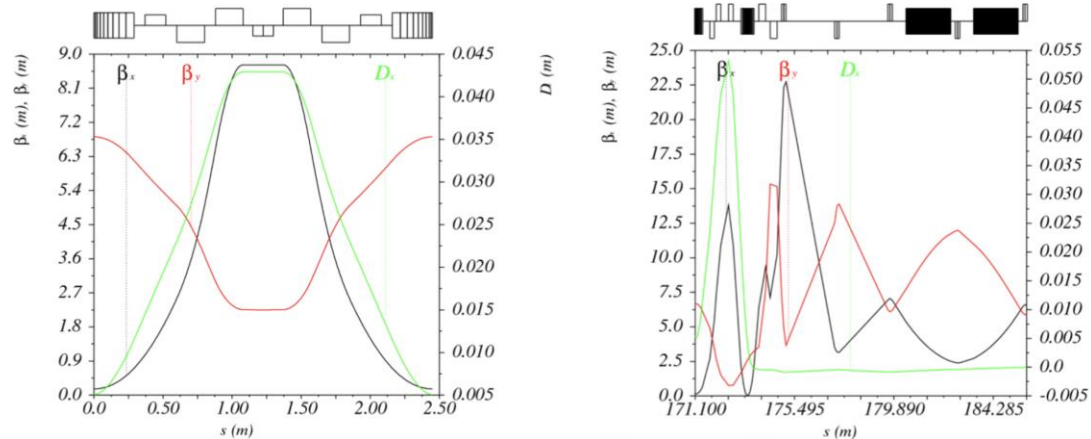
iteration 3

Phosphorous beam profile monitor measurements at the end of the FACET linac, before the dispersion correction, after one iteration step, and after three iteration steps. Iteration zero is before the correction.

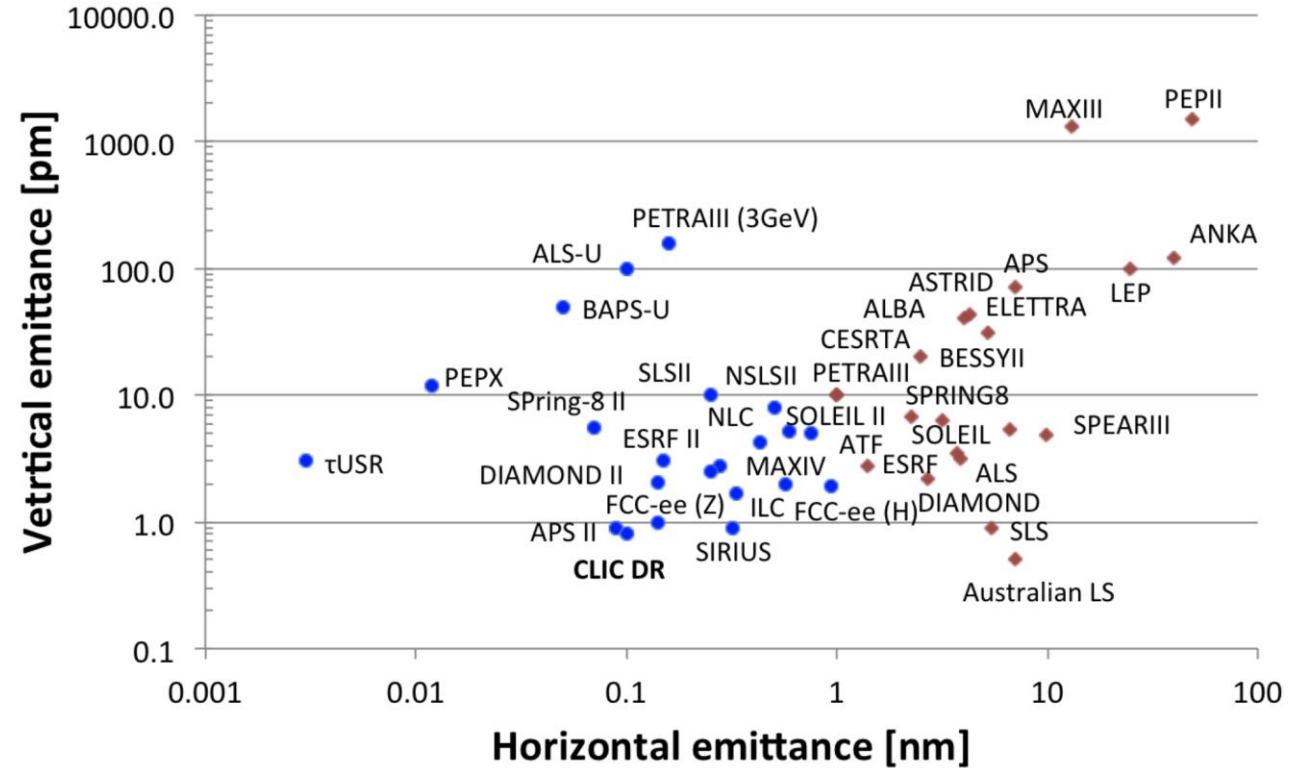
- a) Wakefield plots compared with numerical simulations.
- b) Spectrum of measured data versus numerical simulation.

Damping Rings

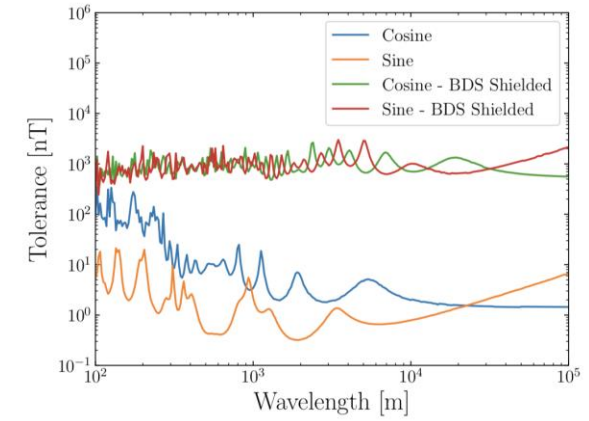
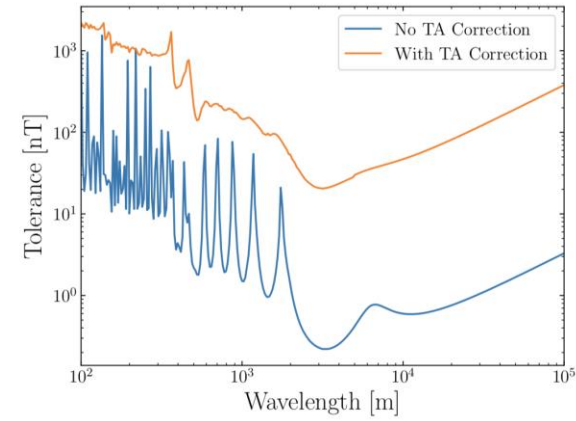
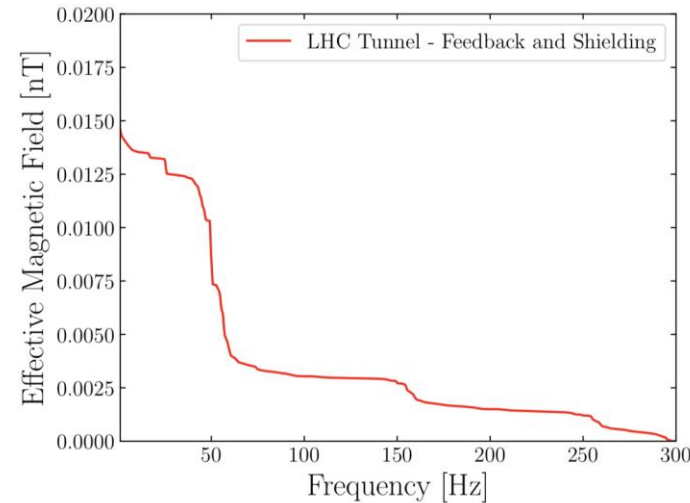
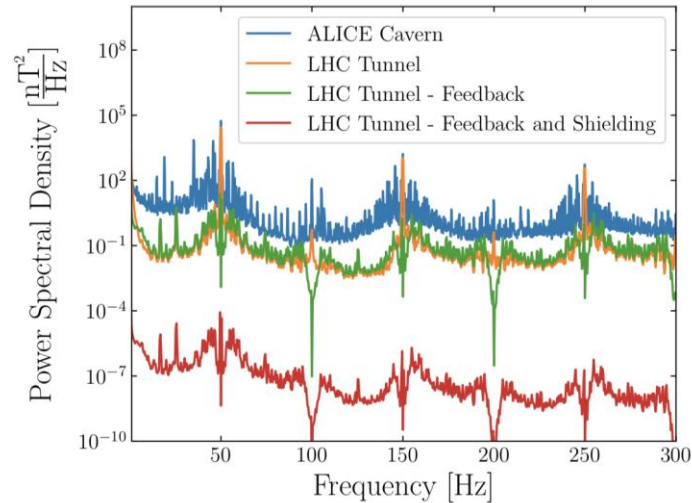
Horizontal versus vertical geometrical emittance of low emittance rings in operation (red) and design (blue). Optical functions of the TME cell (left) and of the dispersion suppressor-beta matching section followed by the FODO cell (right), when using in the arcs the trapezium dipole profiles.



Horizontal versus vertical geometrical emittance of low emittance rings in operation (red) and design (blue).



Impact of Stray Magnetic Fields



Tolerances. (a) RTML long transfer line. (b) ML and ($L^* = 6$ m) BDS.

On the left is the average total power spectral density of the background magnetic field measured at 8 different locations in the LHC tunnel and ALICE detector cavern along with the effective reduction in power due to the currently designed beam-based feedback system and a 1 mm mu-metal coating (with a relative magnetic permeability of 10,000) around a beam pipe of radius 1 cm. On the right is the square root of the integrated power spectral density, representing the magnetic field in the LHC tunnel after mitigation.